RSC Advances

PAPER

View Article Online
View Journal | View Issue

Cite this: *RSC Adv.*, 2018, **8**, 4362

Total phenylethanoid glycosides and magnoloside I_a from *Magnolia officinalis* var. *biloba* fruits inhibit ultraviolet B-induced phototoxicity and inflammation through MAPK/NF-κB signaling pathways

Lanlan Ge,[a] Ling Chen,[a] Qigui Mo,[a] Gao Zhou,[a] Xiaoshan Meng[a] and Youwei Wang *[ab]

Received 4th December 2017
Accepted 13th January 2018

DOI: 10.1039/c7ra13033c

rsc.li/rsc-advances

Magnolia officinalis var. *biloba* is used as a traditional medicine in China and as a food additive in the United Kingdom and the European Union. In this study, total phenylethanoid glycosides (TPG) and magnoloside I_a (MI_a) from *M. officinalis* var. *biloba* fruits showed excellent radical scavenging activities and potent inhibition activities against ultraviolet B (UVB)-induced oxidative damage *in vitro*. *In vivo*, TPG and MI_a inhibited UVB-induced skin phototoxicity in mice upon continuous irradiation for 10 days. Changes in the levels of malondialdehyde, catalase, glutathione peroxidase, superoxide dismutase, and hydroxyproline caused by UVB irradiation were remarkably reversed in a dose-dependent manner after treatment with TPG or MI_a. Protein-level analysis further showed that compared with the UVB group, the TPG high-dose group or MI_a group significantly down-regulated MAPK/NF-κB signaling pathways. Therefore, TPG and MI_a possessed a powerful photoprotective property that can be applied in food and antiphototoxicity formulations.

Introduction

Repeated ultraviolet B (UVB) (wavelength range: 280–320 nm) exposure can initiate a photooxidative reaction that destroys the antioxidant status of an organism. Moreover, it can trigger some reactive oxygen species (ROS)-dominant signaling pathways, thus increasing the ROS level in the cell.[1,2] The oxidative stress caused by repeated UVB exposure can make toxic products more stable; then these toxic products can cause injury to skin tissues.[3] More seriously, repeated UVB exposure can cause lipid peroxidation (LPO) and produce toxic products that can speed up further oxidative injury.[4] The significant damage of UVB exposure primarily has various adverse effects on human skin, including erythemas, edemas, sunburn, hyperplastic responses, hyperpigmentation, photoaging, and immune suppression.[5,6] Repeated UVB exposure also causes acute skin inflammation and even skin carcinogenesis.[7] Therefore, suitable and efficient formulations to alleviate UVB-induced phototoxicity are necessary.

Magnolia officinalis var. *biloba* is a kind of deciduous tree in the Magnoliaceae family, distributed over the mountains and valleys of China at altitudes of 300–1500 m.[8,9] The barks of *M. officinalis* var. *biloba*, "Cortex Magnoliae Officinalis" in Latin and "Houpo" in Chinese,[8] are frequently used as a medicinal herb in China and as a food additive in gum and mints in the United Kingdom and European Union.[10,11] Our previous research showed that *M. officinalis* var. *biloba* fruits extract is rich in phenylethanoid glycosides and the isolated phenylethanoid glycosides had significant antioxidant properties.[10] Literature showed that phenylethanoid glycosides are found mainly in Orobanchaceae plants[12,13] and possess different pharmacological properties, including anti-inflammatory, antioxidant, antitumor, antiviral, antibacterial, immunomodulatory, and neuroprotective effects.[14–21] Protective effects against UVB-induced phototoxicity are related to plant extracts which are rich in antioxidants.[22,23] The purpose of this study is to assess the inhibitory activity against UVB-induced phototoxicity and its underlying mechanisms of total phenylethanoid glycosides (TPG) and magnoloside I_a (MI_a) from *M. officinalis* var. *biloba* fruits.

Materials and methods

Plant material

Fruits were picked from the forests of Enshi (Hubei, China; 30°17′51.56″N, 109°28′27.33″E, A: 1545 m). *M. officinalis* var. *biloba* was authenticated by the corresponding author and deposited as a voucher specimen (no. 14610) at the Traditional

[a]*Institute of TCM and Natural Products, School of Pharmaceutical Sciences, Wuhan University, Wuhan 430071, P. R. China. E-mail: wyw@whu.edu.cn; Fax: +86-27-68759010; Tel: +86-27-68759323*

[b]*MOE Key Laboratory of Combinatorial Biosynthesis and Drug Discovery, Wuhan University, Wuhan 430072, P. R. China*

Chinese Medicine Specimen Museum, School of Pharmaceutical Science, Wuhan University, China.

Reagents

Diagnostic kits for malondialdehyde (MDA), superoxide dismutase (SOD), glutathione peroxidase (GPx), hydroxyproline (Hyp), and catalase (CAT) were bought from Nanjing Jiancheng Technology Co., Ltd. (Nanjing, China). The antibodies of β-actin, JNK, p-JNK, IκBα, and p-65 were obtained from Santa Cruz Biotechnology, Inc. (Santa Cruz, CA, USA). COX-2, ERK, p-ERK, and IKKα antibodies were purchased from Cell Signaling Technology (Beverly, MA, USA). The antibodies of p38 and p-p38 were bought from Abcam (Cambridge, UK). Gallic acid (GA), butylated hydroxytoluene (BHT), ascorbic acid (Vc), and other reagents were bought from Sinopharm Chemical Reagent Co., Ltd. (Shanghai, China).

Experimental animals

The animal experiments were approved by the Institutional Animal Ethical Committee, the Committee for the Purpose of Control, and Supervision of Experiments on Animals at Wuhan University (Wuhan, China). Female Sprague Dawley (SD) rats (200 ± 20 g, $n = 10$) and male BALB/c mice (20 ± 2 g, $n = 56$) were bought from the Laboratory Animal Center of Wuhan University, Wuhan, China. All rats and all mice were maintained on a cycle of 12 h light and 12 h dark with a relative humidity of 30–60% at 25 °C ± 2 °C. Standard pellet diets and unlimited purified water were provided for these animals. Animals were acclimatized to the surrounding environment for one week. All experimental procedures conformed to the Regulations for the Administration of Affairs Concerning Experimental Animals of China.

Preparation of TPG and MI_a

TPG were prepared using a previously published method.[10] In brief, the powder of dried *M. officinalis* var. *biloba* fruits was extracted with 70% alcohol (solvent/fruit ratio of 10 : 1, v/w) for 3 h. The alcohol extracts were suspended in pure water and then partitioned with chloroform, ethyl acetate, and *n*-butanol. Based on the pre-experiment, the *n*-butanol fraction (63.4 g) was rich in phenylethanoid glycoside, so it was named TPG. The TPG yield was 1.2% relative to the dry raw material. MI_a was prepared on a preparative HPLC system using our described method,[10] and its purity was more than 98%.

HPLC analysis of TPG

The HPLC analysis of TPG was performed on a Shimadzu LC-20AT system (Shimadzu, Tokyo, Japan), and it was furnished with an SPD-20A UV detector and a binary solvent manager. Diamonsil C18 analytical column (5 μm, 250 mm × 4.6 mm, Dikma Technologies, Beijing, China) was used. Acetonitrile (A) and 0.1% formic acid water (B) were selected as mobile phase. The gradient started from 10% A and altered to 15% A after 10 min, 20% A after 15 min, 30% A after 10 min, and 35% after 5 min. The temperature of the column oven was 25 °C, and 20 μL was injected into the system. The flow rate was 1.0 mL min^{-1}, and UV spectra were collected at 294 nm.

Determination of phenylethanoid glycoside content in TPG

The total phenylethanoid glycoside content in TPG was measured using a method in a previous study.[24] In short, using a detection wavelength of 330 nm and MI_a as a standard, UV spectrophotometry was used to determine phenylethanoid glycoside content in TPG. Experimental results were showed in mg of MI_a equivalents per g of dry extract.

Free radical scavenging assays

The abilities of test samples to scavenge ABTS radical cation ($ABTS^{\bullet+}$) and DPPH were determined as previously described.[22,25] Radical scavenging activities were expressed in the value of half maximal inhibitory concentration (IC_{50}). The capacity to scavenge superoxide anion radicals ($O_2^{-\bullet}$) was tested by a pyrogallol auto-oxidation system.[26] The rate constant (K_b) of automatic oxidation reaction was computed based on the curve of A_{325} nm *versus* time. Vc and BHT were used as positive controls.

In vitro protective activities

Separation of mitochondria. The mitochondria were prepared from SD rats as previously published.[22] Briefly, rat liver was isolated from SD rats and homogenized in 0.25 M sucrose solutions containing 1 mM EDTA. All homogenates were centrifuged at 3000 × *g* for 10 min first and then at 10 000 × *g* for 10 min. The first centrifugation was designed to remove cell debris, whereas the purpose of the second centrifugation was to get sediment mitochondria. All procedures were carried out at 4 °C.

Experimental groups and UVB irradiation. In the reaction system, 0.5 mL mitochondrial protein and 0.1 mL of different TPG concentrations (10, 50 and 100 μg mL^{-1} in 0.05 M phosphate buffer, pH 7.4) were added. The concentration of MI_a groups were designated according to their percentage in the corresponding TPG groups. BHT and GA were the positive control groups, whereas 0.1 mL phosphate buffer was added to the model group but without test sample. The model, BHT, GA, and test compounds groups were placed in an orifice plate at 37 °C and exposed to radiation for 4 h using a 20 W UVB lamp (TL/12RS, Philips). The distance of the lamp to the orifice plate was 15 cm. The blank control had the same ingredients as the model group, but it was not exposed to radiation. The irradiation dose was detected to be 0.88 J cm^{-2} by a UV irradiance meter (UV-340B, Sampo Scientific Instrument Co. Ltd., Shenzhen).

Measurement of MDA and lipid hydroperoxide (LOOH). The level of UVB-induced MDA in the mitochondria from rat liver was tested by measuring the amount of thiobarbituric acid reactive substances using a previously published thiobarbituric acid method.[1] While a previous approach was adjusted to measure the level of LOOH,[22,27] the prevention percentage of MDA and LOOH was computed through the following formula: prevention percentage $= [(A_m - A_s)/(A_m - A_b)] \times 100$. In this case, A_m was the absorbance of the model group, A_s was the absorbance of the sample groups treated with TPG, MI_a, GA, and BHT, and A_b was the absorbance of the blank control group.

In vivo protective activities

Depilation treatment of test animals. For three days before the start of the UVB irradiation experiment, the back furs of all BALB/C mice were clipped by electric shaver. Moreover, the back skin (9 cm^2) were thoroughly dehaired using 8% sodium sulfide.[28,29]

Experimental groups and UVB radiation. The BALB/C mice were randomly separated into seven groups: control group, model group, GA group (200 mg kg^{-1}), TPG low-dose group (50 mg kg^{-1}), TPG medium-dose group (100 mg kg^{-1} body), TPG high-dose group (200 mg kg^{-1}), and MI_a group (110 mg kg^{-1}). Each group contained eight mice. The mice in the control group and model group were treated with the same volume of solvent (0.1% carboxymethylcellulose-Na). All mouse groups, besides the control group, received the same radiation. The radiation height from the 20 W UVB lamp to the back of the mice was set at 15 cm. The UVB irradiation experiment was set for 1 h daily for the first 5 days (irradiation dose was 0.22 J cm^{-2}); another 5 days was set for 2 h daily (irradiation dose was 0.44 J cm^{-2}).[22] All mice received their corresponding group solvent on their back skin for 30 min before UVB exposure.

Measurement of MDA, CAT, GPx, Hyp, and SOD. The skin samples of the mice under irradiation were collected for further analysis. The homogenized skin samples (1 : 9, w/v) were placed in 0 °C saline solution and centrifuged for 15 min at 6000 × *g* at 4 °C. Then, the supernatants were collected and used to analyze the levels of MDA, CAT, GPx, Hyp, and SOD using their corresponding reagent kit.

Histopathological analysis. All skin samples were fixed in 10% neutral buffered formalin. Then, they were embedded in paraffin and sliced into 5 μm-thick sections. Hematoxylin and eosin dye (H&E) was used to stain the sections, and a microscope was used to observe the histopathological changes of these sections.

Immunoblotting analysis. All mouse skin samples were homogenized (1 : 9, w/v) in 0 °C radio immunoprecipitation assay (RIPA) lysis buffer containing a protease inhibitor. Each homogenate was centrifuged at 12 000 × *g* for 10 min at 4 °C, and the supernatants (total protein) were gathered and reserved at −80 °C. Nuclear proteins were isolated using the cytoplasmic and nuclear extraction kit (Wuhan Goodbio Technology Co., Ltd., Wuhan, China). The proteins were isolated by SDS-PAGE and then transferred to a polyvinylidene fluoride membrane. The membrane was then blocked with 5% nonfat milk for one hour in TBS buffer and incubated with corresponding primary antibodies. Results were measured against enhanced chemiluminescence plus western blot (WB) detection reagents.

Statistical analysis

Experimental data were presented as means ± SD in triplicate. Statistical significance was analyzed by least significant difference *post hoc* testing with SPSS 20.0, and $p < 0.05$ was regarded significant.

Results and discussion

HPLC analysis

The main chemical components in TPG were detected at 294 nm by HPLC (Fig. 1) and identified by previous studies.[10,30] They were syringin (1), magnoloside II_a (2), magnoloside II_b (3), MI_a (4), magnoloside III_a (5), magnoloside IV_a (6), magnoloside

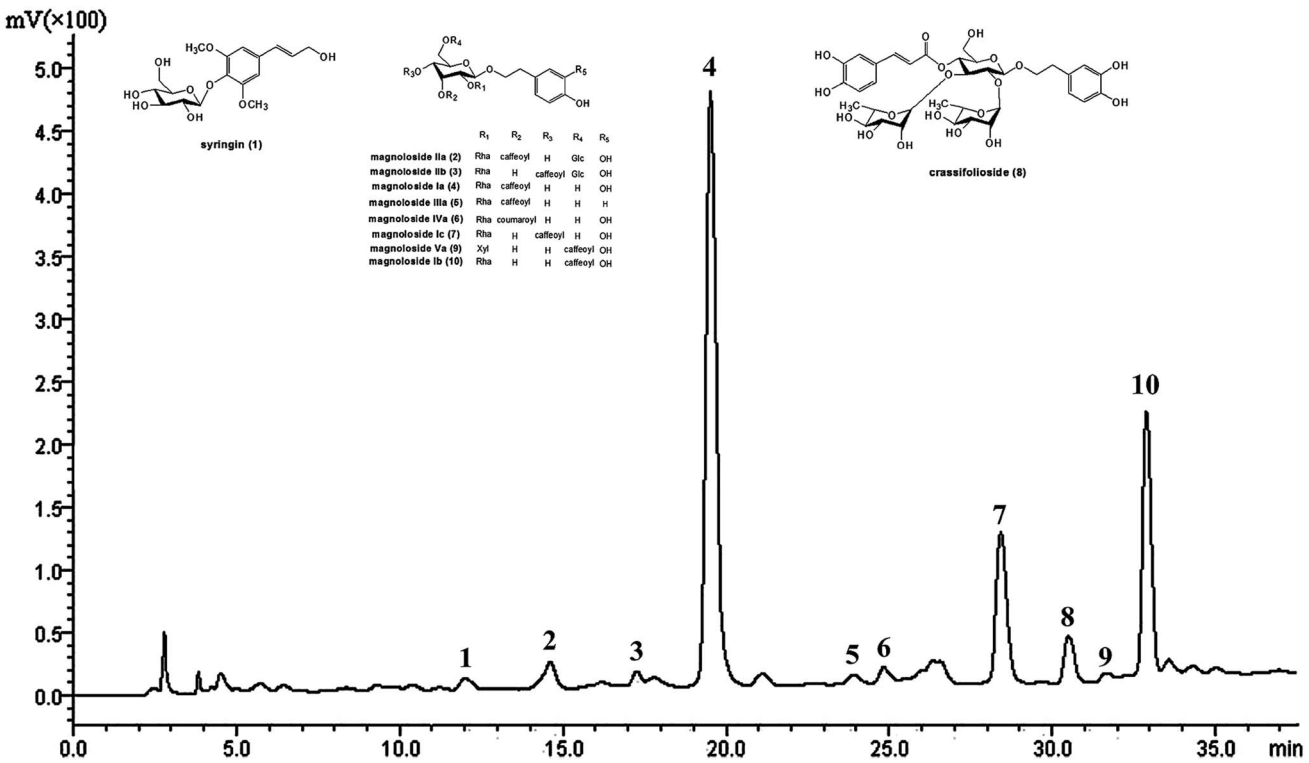

Fig. 1 HPLC chromatogram of TPG at 294 nm. TPG, total phenylethanoid glycosides from *M. officinalis* var. *biloba* fruits.

I_c (7), crassifolioside (8), magnoloside V_a (9), and magnoloside I_b (10). They were typical phenylethanoid glycosides. We concluded that phenylethanoid glycosides are the main active compounds in TPG based on the results of HPLC analysis.

The phenylethanoid glycoside content in TPG

The calibration curve of MI_a showed strong linearity from 4 μg mL^{-1} to 24 μg mL^{-1} with the following regression equation: $Y = 40.799X + 0.04$ ($R^2 = 0.9999$). The average recovery was 95.7% with relative standard deviation (RSD) = 2.1%. Therefore, the method was simple, accurate, and reproducible. According to the equation, the total phenylethanoid glycoside content in TPG was 549.0 ± 10.9 mg of MI_a equivalents per g of dry extract. Results showed that TPG had relatively high phenylethanoid glycoside content.

Table 1 Free radical scavenging activities of TPG and MI_a[a]

	IC_{50} (μg mL^{-1})		K_b ($\times 10^{-4}$ A s^{-1})
Compound	DPPH	ABTS	Superoxide anion
TPG	19.35 ± 0.42[a]	3.43 ± 0.19[c]	14.20 ± 0.15[f]
MI_a	7.35 ± 0.36[b]	2.19 ± 0.07[d]	10.37 ± 0.33[g]
Vc	7.20 ± 0.14[b]	2.03 ± 0.18[d]	0.09 ± 0.02[h]
BHT	19.79 ± 1.01[a]	1.60 ± 0.07[e]	10.40 ± 0.55[g]
Blank	—	—	15.35 ± 0.19[i]

[a] Values were the means ± SD (n = 3); TPG, total phenylethanoid glycosides from *M. officinalis* var. *biloba* fruits; MI_a, magnoloside I_a; Vc, ascorbic acid; BHT, butylated hydroxytoluene. Significant differences ($p < 0.05$) between means are indicated by different letters above the histogram bars. The same letters indicate no significant difference among the different samples.

Free radical scavenging abilities

DPPH, $ABTS^{\bullet+}$, and $O_2^{-\bullet}$, the most common free radicals generated *in vitro*, have been extensively used for the detection of free radical scavenging ability.[1,25,26] Table 1 summarizes the free radical scavenging abilities of TPG and MI_a. In the DPPH assay, TPG showed strong DPPH radical scavenging ability with similar IC_{50} value (19.35 ± 0.42 μg mL^{-1}) to the BHT group (19.79 ± 1.01 μg mL^{-1}). Furthermore, MI_a had better activity than TPG, with an IC_{50} value of 7.35 ± 0.36 μg mL^{-1} that was near the value (7.20 ± 0.14 μg mL^{-1}) of the Vc group. In the $ABTS^{\bullet+}$ assay, the IC_{50} of TPG and MI_a was 3.43 ± 0.19 and 2.19 ± 0.07 μg mL^{-1}, respectively. In the $O_2^{-\cdot}$ assay, the $O_2^{-\bullet}$ scavenging activity of MI_a was weaker than that of Vc but equal to

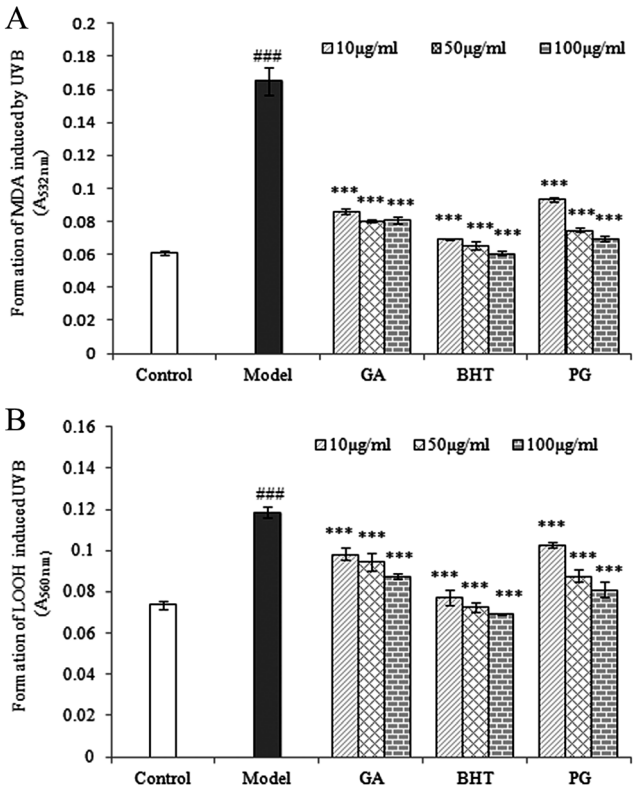

Fig. 2 Effects of TPG on UVB-induced changes in MDA (A) and LOOH (B) levels; data are presented as the mean ± SD (n = 3). TPG, total phenylethanoid glycosides from *M. officinalis* var. *biloba* fruits; GA, gallic acid; BHT, butylated hydroxytoluene; MDA, malondialdehyde; LOOH, lipid hydroperoxide. Symbols represent statistical significance. ###$p < 0.001$, compared with the control group; ***$p < 0.001$, compared with the model group.

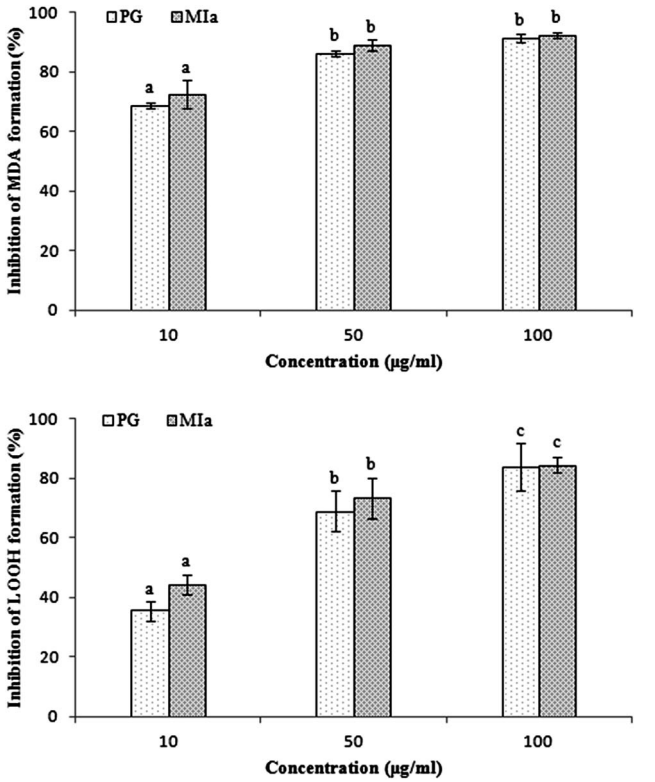

Fig. 3 Comparison of protection of TPG and MI_a on UVB-induced phototoxicity in mitochondria of rat liver (the total phenylethanoid glycoside content in TPG was 55%). (A) Inhibition of MDA formation; (B) inhibition of LOOH formation. Data are presented as the mean ± SD (n = 3). TPG, total phenylethanoid glycosides from *M. officinalis* var. *biloba* fruits; MI_a, magnoloside I_a; MDA, malondialdehyde; LOOH, lipid hydroperoxide. Significant differences ($p < 0.05$) between means are indicated by different letters above the histogram bars. The same letters indicate no significant difference among the different treatments.

Table 2 Effects of TPG and MI_a on body weight in UVB-induced damage mice[a]

Groups	Body weight (g)	
	Day 1	Day 11
Control group	19.07 ± 0.98	23.71 ± 0.84
Model group	19.32 ± 1.11	18.75 ± 0.96###
GA group 200 (mg kg^{-1})	18.86 ± 1.47	20.07 ± 0.98*
TPG-L group 50 (mg kg^{-1})	19.06 ± 1.40	17.74 ± 0.93
TPG-M group 100 (mg kg^{-1})	18.92 ± 1.95	19.11 ± 1.86
TPG-H group 200 (mg kg^{-1})	19.27 ± 1.37	19.71 ± 1.63
MI_a group 110 (mg kg^{-1})	18.91 ± 1.86	20.43 ± 1.70**

[a] Values were mean ± SD (n = 8 animals in each group). Symbols represent statistical significance. TPG, total phenylethanoid glycosides from *M. officinalis* var. *biloba* fruits; MI_a, magnoloside I_a; GA, gallic acid. ###p < 0.001, compared with the control group; *p < 0.05, compared with the model group; **p < 0.01, compared with the model group.

that of BHT. At the same time, TPG also showed a high $O_2^{-\cdot}$ scavenging ability. These data demonstrated that TPG and MI_a can inhibit oxidative stress *in vitro* by scavenging DPPH, $ABTS^{\cdot+}$, and $O_2^{-\cdot}$ free radicals.

In vitro protective activity during repeated UVB exposures

Repeated UVB exposures may lead to mitochondrial damage and LPO. MDA and LOOH are two unstable products of LPO.[6,31] These toxic products cause oxidative stress in the mitochondria, accelerating further damage.[4] To evaluate the protective activity of TPG against phototoxicity caused by UVB, the inhibitory activities of TPG on MDA and LOOH formation were evaluated (Fig. 2). After UVB irradiation for four hours, in comparison with those of the control group (p < 0.001), the levels of MDA and LOOH in the model group were remarkably increased. However, in the TPG groups, GA groups, and BHT groups, the MDA and LOOH levels significantly lower in all concentrations (p < 0.001) (Fig. 2A and B). Similarly, the MI_a groups containing a phenylethanoid glycoside content equivalent to that of the TPG groups also had lower MDA and LOOH levels (Fig. 3). Furthermore, no significant difference was observed between the TPG groups and MI_a groups with the equal content of phenylethanoid glycoside (p > 0.05), as shown in Fig. 3. This finding indicated that TPG played an effective role in preventing photosensitization-induced LPO at various stages, and phenylethanoid glycoside contributed to the protective effect of TPG against UVB-induced phototoxicity.

In vivo protective activity during repeated UVB exposures

MI_a inhibited the loss of body weight caused by repeated UVB exposures. The body weight variations before and after the experiment are shown in Table 2. On the first day of the experiment, no significant difference was observed among the body weights of each mouse group (p > 0.05). On the eleventh day, in comparison with that of the control group (23.71 ± 0.84 g) (p < 0.001), the body weight of the UVB model group (18.75 ± 0.96 g) significantly reduced. The loss of body weight was significantly inhibited after treatment with MI_a (p < 0.01). In particular, the GA group at a concentration of 200 mg kg^{-1} (20.07 ± 0.98 g) and MI_a group at a concentration of 110 mg kg^{-1} (20.43 ± 1.70 g) showed significant inhibition capacity against the body weight loss caused by UVB irradiation (p < 0.05). This finding indicated that repeated UVB exposures led to loss of body weight in mice, whereas MI_a efficiently suppressed such loss in mice.

MI_a inhibited skin hyperplasia caused by repeated UVB exposures. Repeated UVB exposures lead to the dilation of dermal blood vessels, leukocyte infiltration, cutaneous edema, erythema, hyperplasia, and vascular hyperpermeability.[32] H&E staining (Fig. 4) revealed that the epithelial thickness of the mouse skin was definitely increased after repeated UVB exposures. Interestingly, this skin hyperplasia caused by repeated UVB exposures was improved after treatment with MI_a.

TPG or MI_a inhibited skin oxidative damage caused by repeated UVB exposures. Repeated UVB exposures generate a lot of ROS and lead to oxidative skin damage and thus further generate oxidative stress. MDA caused by ROS is regarded as one of the most significant secondary oxidation products of oxidative stress.[33] Meanwhile, antioxidant enzymes, including CAT, GPx, and SOD, are used to protect against oxidative stress and tissue damage. These enzymes play an important role in the defense against the adverse impacts caused by free radicals and ROS in biological systems.[22,34–36] Many studies demonstrated

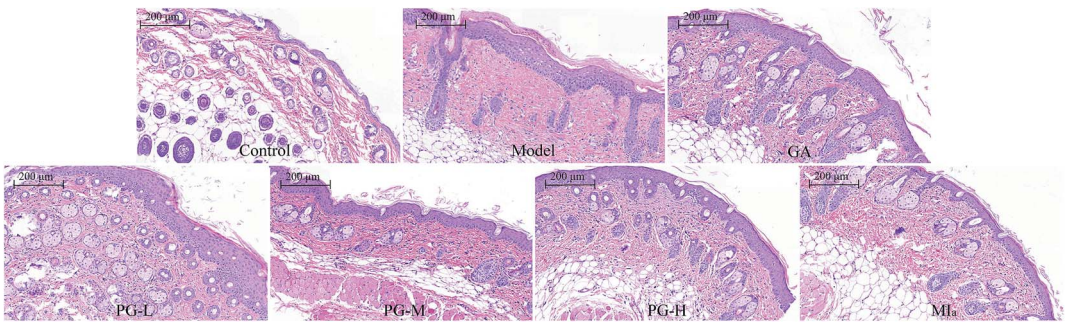

Fig. 4 Sections of back skin tissue of UVB-induced damage in mice (H&E staining, ×100). TPG, total phenylethanoid glycosides from *M. officinalis* var. *biloba* fruits; MI_a, magnoloside I_a; GA, gallic acid; control group; model group; GA group 200 (mg kg^{-1}); TPG-L group 50 (mg kg^{-1}); TPG-M group 100 (mg kg^{-1}); TPG-H group 200 (mg kg^{-1}); MI_a group 110 (mg kg^{-1}).

Table 3 The variation of MDA, CAT, GPx, SOD and Hyp in skin tissue of mice exposed to UVB in the presence and absence of TPG and MI_a[a]

Groups	Skin tissue				
	MDA (nmol mg^{-1} protein)	CAT (U g^{-1} protein)	GPx (U mg^{-1} protein)	SOD (U mg^{-1} protein)	Hyp (μg mg^{-1} protein)
Control group	6.43 ± 0.93	47.67 ± 10.26	90.82 ± 21.60	368.68 ± 54.31	2.23 ± 0.43
Model group	8.53 ± 0.85###	14.97 ± 4.75###	61.61 ± 14.35###	205.63 ± 27.25###	1.70 ± 0.25###
GA group 200 (mg kg^{-1})	5.69 ± 1.72***	37.80 ± 3.03***	88.99 ± 5.22***	335.68 ± 32.98***	2.09 ± 0.18***
TPG-L group 50 (mg kg^{-1})	7.37 ± 0.77*	15.51 ± 1.99	80.62 ± 5.56**	220.59 ± 18.63	1.75 ± 0.15
TPG-M group 100 (mg kg^{-1})	6.98 ± 1.20**	24.74 ± 3.81***	90.10 ± 5.92***	281.48 ± 18.34***	1.83 ± 0.12
TPG-H group 200 (mg kg^{-1})	6.48 ± 0.62***	38.75 ± 3.81***	93.43 ± 6.50***	316.10 ± 33.87***	1.97 ± 0.14*
MI_a group 110 (mg kg^{-1})	6.21 ± 1.18***	41.12 ± 5.70***	95.82 ± 12.93***	332.29 ± 30.41***	2.07 ± 0.15**

[a] Values were mean ± SD ($n = 8$ animals in each group). Symbols represent statistical significance. TPG, total phenylethanoid glycosides from *M. officinalis* var. *biloba* fruits; MI_a, magnoloside I_a; GA, gallic acid; MDA, malondialdehyde; CAT, catalase; GPx, glutathione peroxidase; SOD, superoxide dismutase; Hyp, hydroxyproline. ###$p < 0.001$ compared with the control group; *$p < 0.05$ compared with the model group, **$p < 0.01$ compared with the model group, ***$p < 0.001$ compared with the model group.

that free radical scavengers have the potential to effectively lessen UVB-induced phototoxicity.[37,38] The influence of TPG and MI_a on the levels of MDA, CAT, GPx, SOD and Hyp in mice repeatedly exposed to UVB was evaluated in this study (Table 3). The UVB model group exhibited a remarkable decrease in their levels of CAT (14.97 ± 4.75 U g^{-1} protein), GPx (61.61 ± 14.35 U mg^{-1} protein), and SOD (205.63 ± 27.25 U mg^{-1} protein), together with a remarkable rise in the content of MDA (8.53 ± 0.85 nmol mg^{-1} protein) in compared the control group ($p < 0.001$). In the presence of MI_a and higher doses of TPG levels of enzymes were better heightened compared to the model group. Our results clearly demonstrated that TPG or MI_a possessed favorable protective effects against UVB-induced oxidative damage by increasing the levels of CAT, GPx, and SOD and by decreasing MDA formation.

The level of Hyp can be measured to estimate the level of collagen. Collagen is one of the most crucial structural proteins of the skin. The reduction in the content of Hyp is seen as wrinkle formation in photoaged skin.[28] As shown in Table 3, in comparison with that of the control group ($p < 0.001$), the model group showed a remarkable decrease in Hyp level (1.70 ± 0.25 μg mg^{-1} protein), and the change was remarkably reversed when the mice were treated with GA (200 mg kg^{-1}), TPG (200 mg kg^{-1}), or MI_a (110 mg kg^{-1}) ($p < 0.05$). Our results demonstrated that treatment with TPG or MI_a effectively prevented wrinkle formation caused by repeated UVB exposures.

TPG or MI_a inhibited inflammation caused by repeated UVB exposures. ROS is generated by UVB irradiation in a direct and straightforward way. Moreover, the body's antioxidant defense system is depleted, and an aggrandized oxidative damage emerges due to the effect of the inflammatory response.[39] ROS is responsible for many diversified oxidative-stress-related diseases as well as inflammation, including skin cancer and aging.[40] Reduplicated UVB exposures brings about the overexpression of proinflammatory enzymes iNOS and COX-2 and cytokines TNF-α and IL-6, as mentioned in previous studies.[32,41] COX-2 plays an important role in UVB-induced inflammation because it catalyzes the production of PGE_2 from prostanoid precursors.[42] Furthermore, a few animal models on inflammation have verified the overexpression of COX-2.[43,44] The influence of TPG and MI_a on the UVB-induced expression of COX-2 protein in skin tissue was assessed during this study. WB analysis revealed that repeated UVB exposures led to

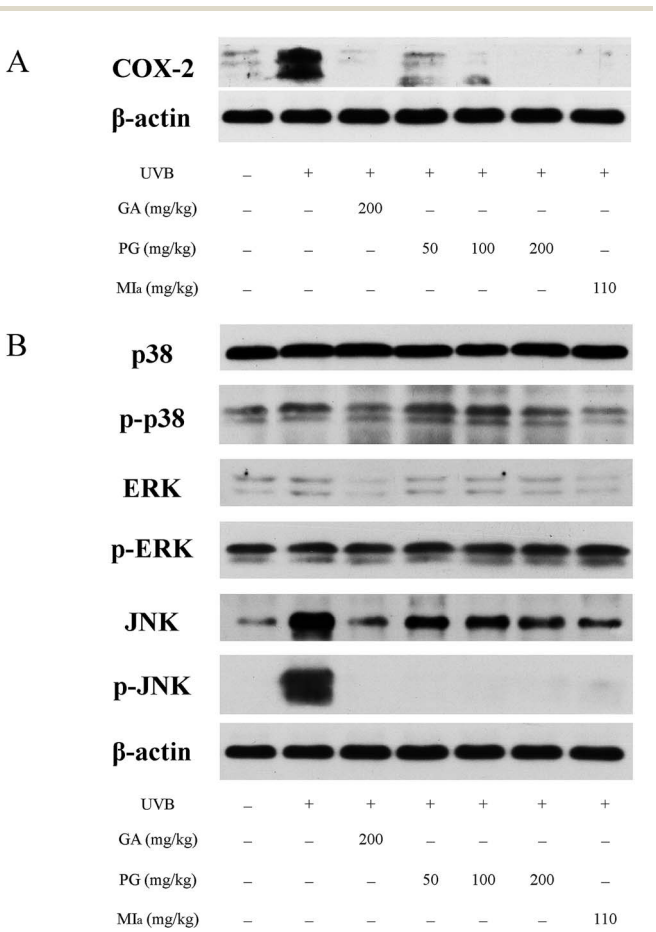

Fig. 5 Effects of TPG and MI_a on protein expressions of COX-2 (A) and MAPKs (B) in the back-skin tissue of mice with UVB-induced damage. TPG, total phenylethanoid glycosides from *M. officinalis* var. *biloba* fruits; MI_a, magnoloside I_a; GA, gallic acid.

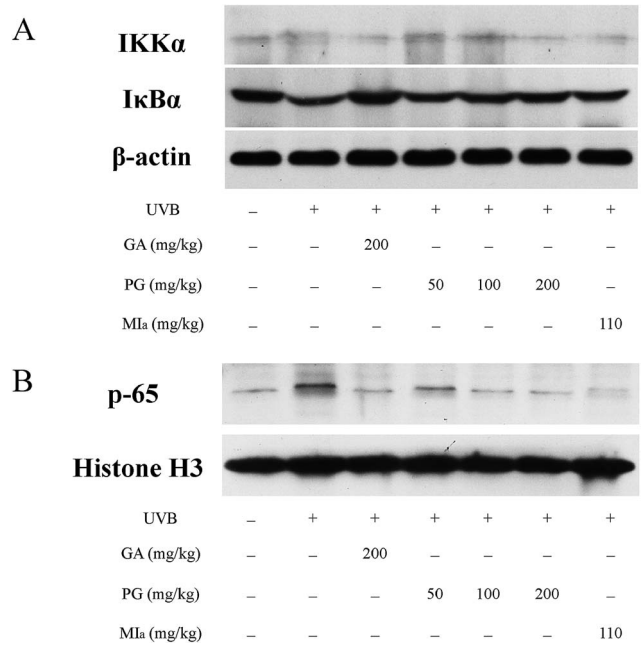

Fig. 6 Effects of TPG and MI_a on protein expressions of IKKα, IκBα (A) and p65 (B) in the back-skin tissue of mice with UVB-induced damage. TPG, total phenylethanoid glycosides from *M. officinalis* var. *biloba* fruits; MI_a, magnoloside I_a; GA, gallic acid.

a remarkable increase in the overexpression of COX-2 protein in the control group (Fig. 5A). However, the expression of COX-2 protein in TPG or MI_a groups was decreased in contrast with that of mice whose skin was exposed to UVB irradiation alone. Therefore, we concluded that TPG or MI_a inhibited inflammation by reducing the level of COX-2 protein.

TPG or MI_a inhibited the phosphorylation of MAPK protein caused by repeated UVB exposures. MAPK proteins are made up of three family members, including Jun N-terminal kinases (JNK), p38 kinase, and extracellular signal-regulated protein kinase (ERK).[45,46] Oxidative stress caused by UVB irradiation plays an important role in the activation of phosphorylated MAPK protein, including ERK, JNK, and p38. These phosphorylated-MAPK (p-MAPK) proteins are involved in phototoxicity.[47,48] Furthermore, MAPK and p-MAPK proteins are proven to modulate NF-κB activation.[32] In this study, we also analyzed the MAPK and p-MAPK expressions upon treatment with TPG and MI_a. As shown in Fig. 5B, WB analysis elucidated that repeated UVB exposures to mouse skin led to increasing levels of phosphorylation of ERK, JNK, and p38. Meanwhile, TPG high-dose group and MI_a groups inhibited the activation of p-p38 and p-JNK. This study demonstrated that TPG or MI_a inhibited the UVB-induced activation of MAPK and p-MAPK on mouse skin, thereby reducing the risk of phototoxicity.

TPG or MI_a inhibited the activation of NF-κB pathway caused by repeated UVB exposures. Repeated UVB exposures lead to the activation of NF-κB pathway,[49] and p65 is the downstream target of this pathway.[50] UVB irradiation triggers the activation of IKK, which causes the phosphorylation of serine residues in IκBα and then leads to the degradation of IκBα protein, followed by translocation and activation of p65 to the nucleus.[51,52] The activation of NF-κB pathway caused by repeated UVB exposures stimulates inflammatory cytokine expressions that contribute to skin inflammation.[49] As shown in Fig. 6A, the cytoplasmic levels of activated IKKα were lower in the TPG high-dose group and MI_a group in comparison with those of the UVB model group, and the cytoplasmic levels of IκBα protein were the opposite. At the same time, our results also indicated that TPG markedly reduced UVB-induced p65 activation, and MI_a also had such inhibition effect (Fig. 6B). To sum up, we concluded that TPG and MI_a inhibited the nuclear translocation of UVB-induced p65 protein by preventing the activation of IKKα and the succeeding degradation of IκBα protein in mouse skin.

Conclusion

In conclusion, TPG and MI_a efficiently scavenged free radicals and prevented the UVB-induced LPO at its various stages *in*

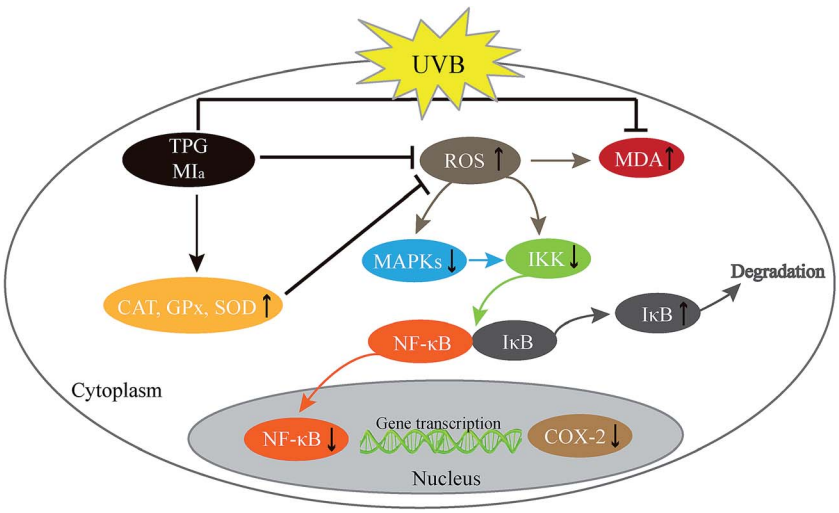

Fig. 7 Proposed mechanism of photoprotection by TPG and MI_a. TPG, total phenylethanoid glycosides from *M. officinalis* var. *biloba* fruits; MI_a, magnoloside I_a.

vitro. MI_a treated mice had less skin thickening, lower MDA levels, maintained better GPx, CAT, SOD, and Hyp levels, and increased body weights indicating enhanced protection against UVB-induced phototoxicity. Furthermore, TPG and MI_a also prevented inflammation by inhibiting the activation of MAPK/NF-κB signaling pathways. The proposed mechanism involved the reduction of p-MAPK levels and dephosphorylation of serine residues in IκBα by IKK, thereby resulting in the deactivation of NF-κB and COX-2 (Fig. 7). Furthermore, our experimental results also demonstrated that the protective effect of TPG against UVB-induced phototoxicity was generally associated with the presence of phenylethanoid glycoside. Based on this study, we suggested that TPG and MI_a can be used as photoprotective agents in food products due to their free radical scavenging and anti-inflammatory activities. This study is expected to provide additional value to *M. officinalis* var. *biloba* fruits and may be helpful for its applications in the scientific field.

Conflicts of interest

The authors declare no competing financial interest.

Acknowledgements

This work was supported by the Project of the National Twelve-Five Year Research Program of China (2011BAI06B06; 2012BAI29B03), the Commonweal Specialized Research Fund of China Agriculture (201103016), and the Nanjing 321 Plan for Bringing in Technological Leading Talents (2013A12011).

References

1 B. X. Ma, L. Zhu, X. Y. Zang, Y. X Chen, D. Li and Y. W. Wang, *Coptis chinensis* inflorescence and its main alkaloids protect against ultraviolet-B-induced oxidative damage, *J. Funct. Foods*, 2013, **5**, 1665–1672.

2 V. A. Trabosh, A. Daher, K. A. Divito, K. Amin, C. M. Simbulan-Rosenthal and D. S. Rosenthal, UVB upregulates the bax promoter in immortalized human keratinocytes via ROS induction of Id3, *Exp. Dermatol.*, 2009, **18**, 387–395.

3 M. Abu Zaid, F. Afaq, D. N. Syed, M. Dreher and H. Mukhtar, Inhibition of UVB mediated oxidative stress and markers of photoaging in immortalized HaCaT keratinocytes by pomegranate polyphenol extract POMx, *Photochem. Photobiol.*, 2007, **83**, 882–888.

4 L. Zhu, B. Huang, X. Q. Ban, J. S. He, Y. X. Chen, L. Han and Y. W. Wang, *Coptis chinensis* inflorescence extract protection against ultraviolet-B-induced phototoxicity, and HPLC-MS analysis of its chemical composition, *Food Chem. Toxicol.*, 2012, **50**, 2584–2588.

5 S. Choi, S. K. Lee, J. E. Kim, M. H. Chung and Y. I. Park, Aloesin inhibits hyperpigmentation induced by UV radiation, *Clin. Exp. Dermatol.*, 2002, **27**, 513–515.

6 H. M. Park, E. Moon, A. J. Kim, M. H. Kim, S. Lee, J. B. Lee, Y. K. Park, H. S. Jung, Y. B. Kim and S. Y. Kim, Extract of *Punica granatum* inhibits skin photoaging induced by UVB irradiation, *Int. J. Dermatol.*, 2010, **49**, 276–282.

7 Y. Sano and J. M. Park, Loss of epidermal p38α signaling prevents ultraviolet radiation-induced inflammation *via* acute and chronic mechanisms, *J. Invest. Dermatol.*, 2014, **134**, 2231–2240.

8 Chinese Pharmacopoeia Commission, *Pharmacopoeia of the People's Republic China*, China Medical Science Press, Beijing, China, 2015, vol. 1, pp. 251–252.

9 J. S. He, L. Chen, Y. Si, B. Huang, X. Q. Ban and Y. W. Wang, Population structure and genetic diversity distribution in wild and cultivated populations of the traditional Chinese medicinal plant *Magnolia officinalis* subsp. *biloba* (Magnoliaceae), *Genetica*, 2009, **135**, 233–243.

10 L. L. Ge, W. H. Zhang, G. Zhou, B. X. Ma, Q. G. Mo, Y. X. Chen and Y. W. Wang, Nine phenylethanoid glycosides from *Magnolia officinalis* var. *biloba* fruits and their protective effects against free radical-induced oxidative damage, *Sci. Rep.*, 2017, **7**, 45342.

11 M. Greenberg, P. Urnezis and M. Tian, Compressed mints and chewing gum containing magnolia bark extract are effective against bacteria responsible for oral malodor, *J. Agric. Food Chem.*, 2007, **55**, 9465–9469.

12 L. Li, R. Tsao, R. Yang, C. M. Liu, J. C. Young and H. H. Zhu, Isolation and purification of phenylethanoid glycosides from *Cistanche deserticola* by high-speed counter-current chromatography, *Food Chem.*, 2008, **108**, 702–710.

13 Y. Li, G. Zhou, Y. Peng, P. Tu and X. Li, Screening and identification of three typical phenylethanoid glycosides metabolites from *Cistanches Herba* by human intestinal bacteria using UPLC/Q-TOF-MS, *J. Pharm. Biomed. Anal.*, 2016, **118**, 167–176.

14 H. Bardakci, H. Skaltsa, T. Milosevic-Ifantis, D. Lazari, D. Hadjipavlou-Litina, E. Yesilada and H. Kırmızıbekmez, Antioxidant activities of several Scutellaria taxa and bioactive phytoconstituents from *Scutellaria hastifolia* L., *Ind. Crops Prod.*, 2015, **77**, 196–203.

15 Y. Jiang, S. Mao, W. Huang, B. Lu, Z. Cai, F. Zhou, M. Li, T. Lou and Y. Zhao, Phenylethanoid glycoside profiles and antioxidant activities of *Osmanthus fragrans* Lour. flowers by UPLC/PDA/MS and simulated digestion model, *J. Agric. Food Chem.*, 2016, **64**, 2459–2466.

16 Y. L. Liu, W. J. He, L. Mo, M. F. Shi, Y. Y. Zhu, S. Pan, X. R. Li, Q. M. Xu and S. L. Yang, Antimicrobial, anti-inflammatory activities and toxicology of phenylethanoid glycosides from *Monochasmasa vatieri* Franch. ex Maxim., *J. Ethnopharmacol.*, 2013, **149**, 431–437.

17 Y. G. Liu, X. X. Li, D. C. Xiong, B. Yu, X. Pu and X. S. Ye, Synthetic phenylethanoid glycoside derivatives as potent neuroprotective agents, *Eur. J. Med. Chem.*, 2015, **95**, 313–323.

18 Q. G. Ma, Y. C. Guo, W. M. Liu, Z. Q. Wang, W. T. Mao, X. Zhang, L. T. Yu, Q. C. Yang and R. R. Wei, Phenylethanoid glycosides from *Houttuynia cordata* and their hepatoprotective activities, *Chem. Nat. Compd.*, 2016, **52**, 761–763.

19 J. N. Oyourou, S. Combrinck, T. Regnier and A. Marston, Purification, stability and antifungal activity of verbascoside from *Lippia javanica* and *Lantana camara* leaf extracts, *Ind. Crops Prod.*, 2013, **43**, 820–826.

20 X. Song, C. Y. Li, Y. Zeng, H. Q. Wu, Z. Huang, J. Zhang, R. S. Hong, X. X. Chen, L. Y. Wang, X. P. Hu, W. W. Su, Y. Li and Z. D. He, Immunomodulatory effects of crude phenylethanoid glycosides from, *J. Ethnopharmacol.*, 2012, **144**, 584–591.

21 Z. Xue and B. Yang, Phenylethanoid glycosides: Research advances in their phytochemistry, pharmacological activity and pharmacokinetics, *Molecules*, 2016, **21**, 991–1016.

22 B. Huang, L. Zhu, S. Liu, D. Li, Y. X. Chen, B. X. Ma and Y. W. Wang, *In vitro* and *in vivo* evaluation of inhibition activity of lotus (*Nelumbo nucifera* Gaertn.) leaves against ultraviolet B-induced phototoxicity, *J. Photochem. Photobiol., B*, 2013, **121**, 1–5.

23 M. Perde-Schrepler, G. Chereches, I. Brie, C. Tatomir, I. D. Postescu, L. Soran and A. Filip, Grape seed extract as photochemopreventive agent against UVB induced skin cancer, *J. Photochem. Photobiol., B*, 2013, **118**, 16–21.

24 L. N. Wang, J. Chen, M. H. Yang, S. L. Chen, Y. Shi, Y. Qi and T. N. Liu, Quantitative determination of total phenylethanoid glycosides in Cistanche desertiola, *Northwest Pharm. J.*, 2008, **2**, 67–69.

25 S. M. M. R. Mawalagedera, Z. Q. Ou, A. McDowell and K. L. Gould, Effects of boiling and *in vitro* gastrointestinal digestion on the antioxidant activity of *Sonchus oleraceus* leaves, *Food Funct.*, 2016, **7**, 1515–1522.

26 G. Zhou, Y. X. Chen, S. Liu, X. C. Yao and Y. W. Wang, *In vitro* and *in vivo* hepatoprotective and antioxidant activity of ethanolic extract from *Meconopsis integrifolia* (Maxim.) Franch, *J. Ethnopharmacol.*, 2013, **148**, 664–670.

27 N. Z. Jaffar, T. S. Javad, B. H. Ines and P. W. Simon, Measurement of hydroperoxides in edible oils using the ferrous oxidation in xylenol orange assay, *J. Agric. Food Chem.*, 1995, **43**, 17–21.

28 H. Hou, B. F. Li, Y. L. Zhuang, G. Y. Ren, M. Y. Yan, Y. P. Cai, X. K. Zhang and L. Chen, The effect of pacific cod (Gadus macrocephalus) skin gelatin polypeptides on UV radiation-induced skin photoaging in ICR mice, *Food Chem.*, 2009, **115**, 945–950.

29 M. Sumiyoshi and Y. Kimura, Effects of olive leaf extract and its main component oleuropein on acute ultraviolet B irradiation-induced skin changes in C57BL/6J mice, *Phytother. Res.*, 2010, **24**, 995–1003.

30 S. X. Yu, R. Y. Yan, R. X. Liang, W. Wang and B. Yang, Bioactive polar compounds from stem bark of Magnolia officinalis, *Fitoterapia*, 2012, **83**, 356–361.

31 S. Bhattacharya, J. P. Kamat, S. K. Bandyopadhyay and S. Chattopadhyay, Comparative inhibitory properties of some Indian medicinal plant extracts against photosensitization-induced lipid damage, *Food Chem.*, 2009, **113**, 975–979.

32 S. D. Sharma and S. K. Katiyar, Dietary grape seed proanthocyanidins inhibit UVB induced cyclooxygenase-2 expression and other inflammatory mediators in UVB exposed skin and skin tumors of SKH-1 hairless mice, *Pharm. Res.*, 2010, **27**, 1092–1102.

33 N. Khan, D. N. Syed, H. C. Pal, H. Mukhtar and F. Afaq, Pomegranate fruit extract inhibits UVB-induced inflammation and proliferation by modulating NF-κB and MAPK signaling pathways in mouse skin, *Photochem. Photobiol.*, 2012, **88**, 1126–1134.

34 J. Eliza, P. Daisy and S. Ignacimuthu, Antioxidant activity of constunolide and eremanthin isolated from *Costus speciosus* (Koen ex Retz) Sm, *Chem.-Biol. Interact.*, 2010, **188**, 467–472.

35 F. C. Lidon and J. C. Ramalho, Impact of UV-B irradiation on photosynthetic performance and chloroplast membrane components in *Oryza sativa* L., *J. Photochem. Photobiol., B*, 2011, **104**, 457–466.

36 Z. F. Skalická, F. Zölzer, L. Beránek and J. Racek, Indicators of oxidative stress after ionizing and/or non-ionizing radiation: superoxide dismutase and malondialdehyde, *J. Photochem. Photobiol., B*, 2012, **117**, 111–114.

37 C. W. Lee, H. H. Ko, C. Y. Chai, W. T. Chen, C. C. Lin and F. L. Yen, Effect of artocarpus communis extract on UVB irradiation-induced oxidative stress and inflammation in hairless mice, *Int. J. Mol. Sci.*, 2013, **14**, 3860–3873.

38 M. Sumiyoshi and Y. Kimura, Effects of a turmeric extract (*Curcuma longa*) on chronic ultraviolet B irradiation-induced skin damage in melanin-possessing hairless mice, *Phytomedicine*, 2009, **16**, 1137–1143.

39 A. Petrova, L. M. Davids, F. Rautenbach and J. L. Marnewick, Photoprotection by honeybush extracts, hesperidin and mangiferin against UVB-induced skin damage in SKH-1 mice, *J. Photochem. Photobiol., B*, 2011, **103**, 126–139.

40 F. Afaq, V. M. Adhami and N. Ahmad, Prevention of short-term ultraviolet B radiation-mediated damages by resveratrol in SKH-1 hairless mice, *Toxicol. Appl. Pharmacol.*, 2003, **186**, 28–37.

41 J. A. Lee, B. G. Jung, T. H. Kim, S. G. Lee, Y. S. Park and B. J. Lee, Dietary feeding of *Opuntia humifusa* inhibits UVB radiation-induced carcinogenesis by reducing inflammation and proliferation in hairless mouse model, *Photochem. Photobiol.*, 2013, **89**, 1208–1215.

42 S. M. Fischer, A. Pavone, C. Mikulec, R. Langenbach and J. E. Rundhaug, Cyclooxygenase-2 expression is critical for chronic UV-induced murine skin carcinogenesis, *Mol. Carcinog.*, 2007, **46**, 363–371.

43 P. Pratheeshkumar and G. Kuttan, *Cardiospermumhalicacabum* inhibits cyclophosphamide induced immunosuppression and oxidative stress in mice and also regulates iNOS and COX-2 gene expression in LPS stimulated macrophages, *Asian Pac J Cancer Prev.*, 2010, **11**, 1245–1252.

44 P. Pratheeshkumar and G. Kuttan, Modulation of immune response by *Vernonia cinerea* L. inhibits the proinflammatory cytokine profile, iNOS, and COX-2 expression in LPS-stimulated macrophages, *Immunopharmacol. Immunotoxicol.*, 2011, **33**, 73–83.

45 J. G. Einspahr, B. G. Timothy, D. S. Alberts, N. McKenzie, K. Saboda and J. Warneke, Cross-validation of murine UV signal transduction pathways in human skin, *Photochem. Photobiol.*, 2008, **84**, 463–476.

46 M. Moriyama, H. Moriyama, J. Uda, H. Kudo, Y. Nakajima, A. Goto, T. Moria and T. Hayakawa, BNIP3 upregulation *via* stimulation of ERK and JNK activity is required for the protection of keratinocytes from UVB-induced apoptosis, *Cell Death Dis.*, 2017, **8**, e2576.

47 S. E. Dickinson, E. R. Olson, J. Zhang, S. J. Cooper, T. Melton, P. J. Criswell, A. Casanova, Z. Dong, C. Hu, K. Saboda, E. T. Jacobs, D. S. Alberts and G. T. Bowden, P38 MAP kinase plays a functional role in UVB-induced mouse skin carcinogenesis, *Mol. Carcinog.*, 2011, **50**, 469–478.

48 H. P. Li, Z. J. Li, L. Q. Peng, Q. Jiang, E. T. Zhang, B. H. Liang, R. X. Li and H. L. Zhu, *Lycium barbarum* polysaccharide protects human keratinocytes against UVB-induced photodamage, *Free Radical Res.*, 2017, **51**, 200–210.

49 F. T. M. C. Vicentini, T. He, Y. Shao, M. J. V. Fonseca, W. A. Verri Jr, G. J. Fisher and J. Xu, Quercetin inhibits UV irradiation-induced inflammatory cytokine production in primary human keratinocytes by suppressing NF-κB pathway, *J. Dermatol. Sci.*, 2011, **61**, 162–168.

50 S. D. Sharma, S. M. Meeran and S. K. Katiyar, Dietary grape seed proanthocyanidins inhibit UVB-induced oxidative stress and activation of mitogen-activated protein kinases and nuclear factor-κB signaling *in vivo* SKH-1 hairless mice, *Mol. Cancer Ther.*, 2007, **6**, 995–1005.

51 S. K. Mantena and S. K. Katiyar, Grape seed proanthocyanidins inhibit UV-radiation induced oxidative stress and activation of MAPK and NF-κB signaling in human epidermal keratinocytes, *Free Radicals Biol. Med.*, 2006, **40**, 1603–1614.

52 P. Pratheeshkumar and G. Kuttan, Vernolide-A, a sesquiterpene lactone from *Vernonia cinerea*, induces apoptosis in B16F-10 melanoma cells by modulating p53 and caspase-3 gene expressions and regulating NF-κB-mediated Bcl-2 activation, *Drug Chem. Toxicol.*, 2011, **34**, 261–270.